

The effect of resonant magnetic perturbations on the geodesic acoustic mode in MAST

J. R. Robinson,^{1,*} B. Hnat,¹ P. Dura,¹ A. Kirk,² P. Tamain,³ and the MAST Team²

¹*Physics Department, University of Warwick, Coventry, CV4 7AL, UK.*

²*EURATOM/CCFE Fusion Association, Culham Science Centre, Abingdon, OX14 3DB, UK.*

³*Association Euratom/CEA, CEA Cadarache, F-13108 St. Paul-lez-Durance, France*

(Dated: September 9, 2011)

The geodesic acoustic mode (GAM) is detected in the edge plasma of the MAST tokamak using a reciprocating Langmuir probe. The mode is radially localised, with outer limit ≈ 2 cm inside the separatrix, and interacts with the resonant magnetic perturbations (RMP) generated by external coils. A shift in GAM frequency with plasma rotation is found, consistent with the predicted dispersion relation. A rapid suppression of GAM is observed when the GAM can couple to the imposed $n = 3$ magnetic perturbations in the rotating frame. Non-linear coupling to high wave number turbulence is evident, and an increase in power of turbulence fluctuations is seen after GAM suppression.

PACS numbers: 52.55.Fa, 52.35. Ra, 52.30.-q, 52.35.Mw, 52.35.Py

Understanding the interaction between turbulent transport and the large scale flows in magnetically confined plasmas is one of the key aspects in developing future fusion reactors [1, 2]. Turbulence mediates the flux of energy from small scale instabilities to large scale flows which in turn influence global confinement properties. A generic class of drift instabilities [3] is believed to provide a driving mechanism for the turbulence at the edge of a confinement device where steep density and temperature gradients are present. Upon achieving certain amplitudes, turbulent fluctuations can self-organise into zonal flows [4–7]. These zonal flows are linearly stable and thus act as a sink of energy for turbulence [8]. They can further reduce turbulent fluctuations via eddy shearing mechanism [9, 12]. Suppression of turbulence by zonal flow shearing of turbulent eddies is believed to be an important component of the transition from low confinement to a high confinement mode [9, 10]. High confinement mode [11] which provides much higher fusion power yields has been proposed as a main mode of operation for future fusion reactors.

In the context of magnetically confined plasma, zonal flows are defined as radially localised ($k_r \neq 0$) axisymmetric and azimuthally symmetric ($m = n = 0$, where m and n are the poloidal and toroidal mode numbers, respectively) electrostatic potential modes. Their characteristic evolution time is much larger than turbulence evolution timescales. The Geodesic Acoustic Mode (GAM) [13] is then defined as a zonal flow with a non-zero frequency. A GAM results from the compressibility of the zonal flows in toroidal geometry, coupling to a compressible (acoustic) mode with $m = \pm 1$, through the geodesic curvature of the confining magnetic field. These are distinct from the low frequency Ion Acoustic Mode (IAM), which in strong magnetic field is predominantly field aligned. In recent years, GAMs have been observed in many plasmas and across different confinement regimes, underlying the universal aspect of this

large scale mode [14, 15]. These observations are consistent with theoretical predictions for GAMs, confirming their radial localisation, range of frequencies and the coupling of the GAM to high wave number turbulence.

The electromagnetic properties of GAM and their interaction with Alfvénic modes are not well understood, but a limited number of studies have been dedicated to magnetic field signatures of GAMs. Results from a kinetic theory have shown that, for finite poloidal and toroidal mode numbers, these fluctuations can couple to the Alfvén continuum [16]. Work based on stellarator plasmas suggested generation of a zonal magnetic field by zonal flows [17]. Such coupling to magnetic field perturbations would provide an additional channel for turbulent energy dissipation and thus provide an important mechanism for stabilisation of turbulence. In this paper, we present the first analysis of the interaction between GAMs and the resonant magnetic field perturbations which are generated by external coils [18], designed with the aim of controlling Edge Localised Mode (ELM) instabilities on the Mega Amp Spherical Tokamak (MAST) [19].

MAST is a spherical tokamak with a major radius $R_0 \approx 0.85$ m and a minor radius of $a \approx 0.65$ m, magnetic field strength is about 0.5T with the toroidal, B_t , and the poloidal, B_p , field components giving a pitch angle of about 22 degrees at the edge region. The radial magnetic field perturbations induced by the ELM control coils, resonantly couple to the helical confining field generating localised magnetic islands. This results in complex interactions of the plasma with these Resonant Magnetic Perturbations (RMP). We analyse data from several plasma discharges (numbered 21856 to 21860), that were similar in terms of plasma parameters, but which differed in terms of radial magnetic perturbation. These Ohmic heated plasmas had a line average number density, $n \approx 1.5 \times 10^{19} \text{ m}^{-3}$, and plasma current $I_p = 0.4$ MA. The data were collected using a Gunderstrup type

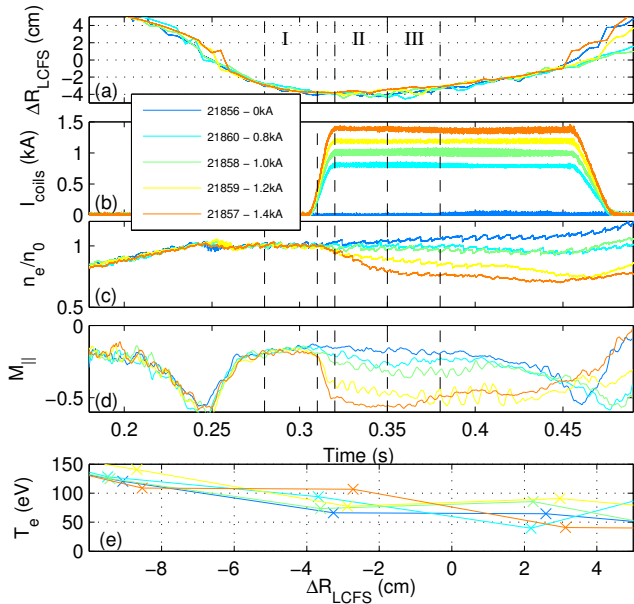


FIG. 1: (a) Langmuir probe position with respect to the last closed flux surface (indicated as 0). (b) ELM coil current (c) line average plasma density normalised to level at $t=0.3s$ (d) Parallel flow Mach number at probe position (e) Thomson scattering temperature profile taken at $t=0.35s$

reciprocating Langmuir probe [21], on the outboard mid-plane, measuring floating potential, ϕ_f as well as a set of ion saturation currents, I_{sat} . As with other studies (see [20], for example) we neglect temperature effects and use floating potential as a proxy for plasma potential.

Figure 1 shows a typical scenario which is applicable to all discharges studied here. Panel (a) of this figure shows the position of the probe with respect to the last closed flux surface (LCFS) as a function of time. The sets of vertical dashed lines indicate three time intervals, marked as I, II and III in the figure, which we will repeatedly refer to in our study. Interval I corresponds to times $t = 0.28 - 0.31$ s when the probe is at a position $r_p = -3.5$ cm inside the LCFS, but before the coils are turned on. Interval II corresponds to times $t = 0.32 - 0.35$ s and position $r_p = -4$ cm, just as the coil current reaches its assigned value, and interval III is the following 30 ms whilst the probe is held at $r_p = -4$ cm, ie. $t = 0.35 - 0.38$ s. The line averaged plasma density for each discharge is shown in Figure 1(c), normalised to the level before the coils turn on, in order to remove the slight shot-to-shot variability due to gas flow rates. We see that the induced RMPs result in a well documented density pump-out [18] which occurs at $t \approx 0.33$ s. Increased plasma rotation is also observed after the magnetic field is perturbed [22]. This is shown in Figure 1(d), where the flow velocity has been calculated using ratios of the fluctuation-averaged I_{sat} signals according to the Van Goubergen model [22]. Finally, in panel (e) we show the edge profiles of elec-

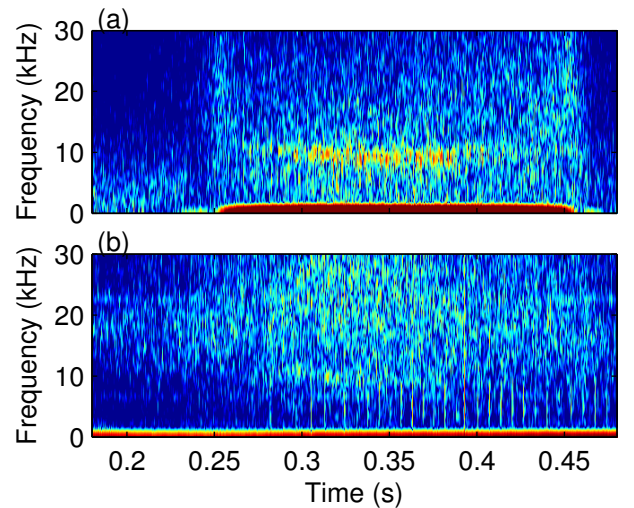


FIG. 2: A representative spectrogram for low frequency part of the spectrum from shot 21856 for (a) potential, showing intermittent high power signature at ≈ 10 kHz frequency, for the period the probe is more than ≈ 2 cm inside the LCFS. (b) Mirnov coil response, showing no corresponding magnetic fluctuation

tron temperature, T_e as measured by the Thomson scattering (TS) technique. All the shots show similar profiles, falling to $T_e \approx 50$ eV at the edge, with a gradient of around 10 eV/cm.

We now present the evidence that the potential perturbations observed at the edge region of MAST are consistent with the GAM theory. Figure 2(a) shows a typical spectrogram of floating potential measurement, when the ELM coils are not activated. A high power feature with frequency of about 10 kHz is clearly visible for a radial location $\Delta R_{LCFS} < -2$ cm for all discharges examined. The distribution of power is not uniform, but rather shows an intermittent characteristic as reported in other observations [14]. It was also noted that peak amplitude in the I_{sat} signal varied with the orientation of pins, with those where the tangent to the probe surface is closest to the field direction showing the strongest response. To strengthen our interpretation of this observed mode, we apply the theoretical GAM dispersion relation [23]:

$$\omega_{GAM}^2 = \frac{\omega_s^2}{2} \left(\lambda + \sqrt{\lambda^2 + \frac{2M^4}{q^2}} \right) \quad (1)$$

to calculate GAM frequency predicted for the plasma of the discharges studied. In the above expression $\omega_s = c_s/R$, $\lambda = 2 + q^{-2} + 4M^2$, sound speed $c_s = \sqrt{T_e/m_i}$, R is the major radius, q is the safety factor and M is the toroidal plasma rotation Mach number. Taking $T_e \approx 80$ eV, as suggested by the TS data shown in Figure 1(e), $q = 6$ from equilibrium reconstruction for our discharges and the major radius of MAST $R_0 = 0.85$ m we

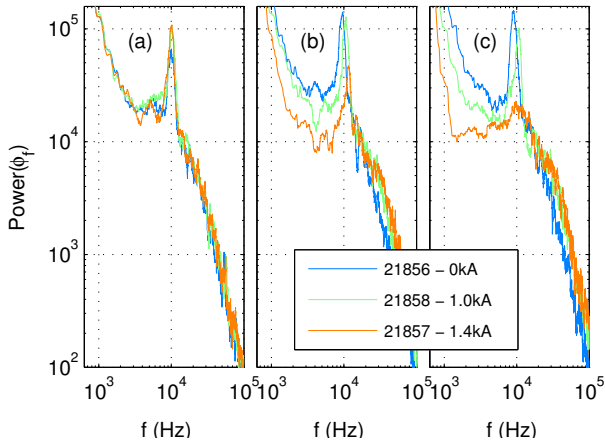


FIG. 3: Power spectral densities for potential fluctuations: (a) interval I: coils off (b) interval II: coils on, peaks shifted (c) interval III: coils on, 30 ms later, peak damped for coil current 1.4 kA.

obtain a GAM frequency $\nu_{\text{GAM}} = \omega_{\text{GAM}}/2\pi = 16.5\text{kHz}$. We see that the expression (1) overestimates the observed frequency, but is reasonably close, considering that it has been derived using a large aspect ratio expansion in $\epsilon = a/R \ll 1$, which is not applicable to spherical tokamaks such as MAST. However, if the radius of the magnetic axis is replaced with radius of the geodesic curvature at the probe position $R_g \approx 1.4\text{ m}$ the predicted frequency coincides with the observed one, $\nu_{\text{GAM}} = 9.9\text{kHz}$. We note that the IAM dispersion relation has an explicit dependence on q^{-1} , and for values used above would give frequency factor of 6 lower than this obtained from (1). We note that there was no other magnetohydrodynamic (MHD) activity during these measurements with comparable frequency. In particular, on close examination of magnetic field signals from the Mirnov coils, such as in Figure 2(b), no evidence of tearing mode perturbations with comparable frequency was found.

Having provided the evidence that the observed potential fluctuations are consistent with the GAM theory we examine the interaction between resonant magnetic perturbations and this acoustic mode. Figure 3(a) shows the power spectrum calculated during the Interval I, before the ELM coil current is switched on. A peak at $\approx 10\text{kHz}$ is clearly visible in this plot and the amplitude of the peak is nearly identical for all discharges considered. These spectra do not saturate for lower frequencies, but show a similar rising trend which strongly suggests that a zero-frequency zonal flow may also be present in the system. At high frequencies spectra exhibit a typical turbulent power-law behaviour. We will later examine the coupling between the GAM and the turbulence.

Figure 3(b) shows the spectra of plasma potential for discharges with three different coil currents, all obtained

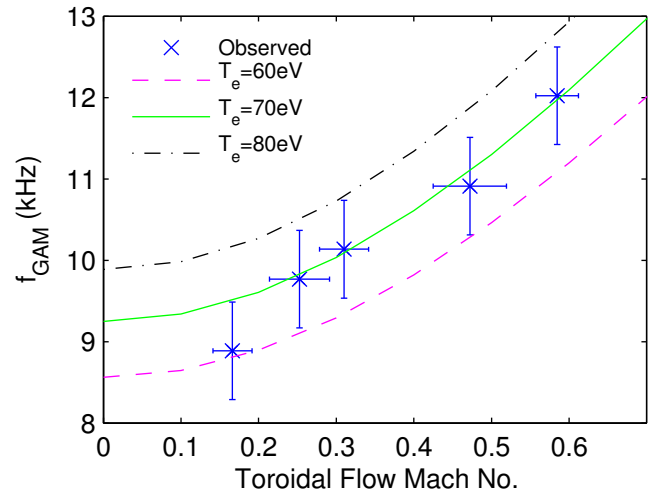


FIG. 4: Observed peak frequency against toroidal spin-up at $R = 1.42\text{ m}$, $q = 6$; together with isotherms for $T_e = 60\text{eV}$, 70eV and 80eV

within interval II. When the ELM coils are turned on the GAM peak is affected in two different ways: the position of the peak is shifted towards higher frequencies with increased coil current and the amplitude of the peak decreases with time. The shift of GAM peak to higher frequencies on the application of RMPs, previously noted in four-field model simulations [24], can be explained by the increased toroidal rotation of the plasma as shown in the Figure 1(d). Here we correlate the shift with the prediction of (1) and find good agreement with the theory when the geodesic radius R_g at the mode location is used in place of the major radius R_0 . The results are shown in the Figure 4. The errorbars correspond to the peak half-maximum width of $\pm 600\text{ Hz}$ and one standard deviation on the mean flow for each shot over interval II.

While frequency shift shows a secular trend with the increased coil current (plasma rotation), the decrease in peak amplitude with time exhibits a threshold-like behaviour. Indeed, Figure 3(c) shows that the most dramatic change occurs when the coil current achieves the value of 1.4 kA. At this point the GAM peak is rapidly damped and disappears entirely within 30ms, as seen in Figure 3(c). Such threshold-like response of GAM to the magnetic perturbations is consistent with other observations on MAST [18, 22].

We believe that this rapid damping of the GAM mode can be explained by its resonant interaction with the imposed RMPs, when considered in the rotating plasma frame. In this rotating frame, GAM will experience the static $n = 3$ magnetic perturbations imposed by the ELM coils as an Alfvénic oscillation with frequency $\omega_{\text{RMP}} = nMc_s/R_g$. Comparing this relation with equation (1), and taking $1/q^2 \ll 1$, a resonance condition is found

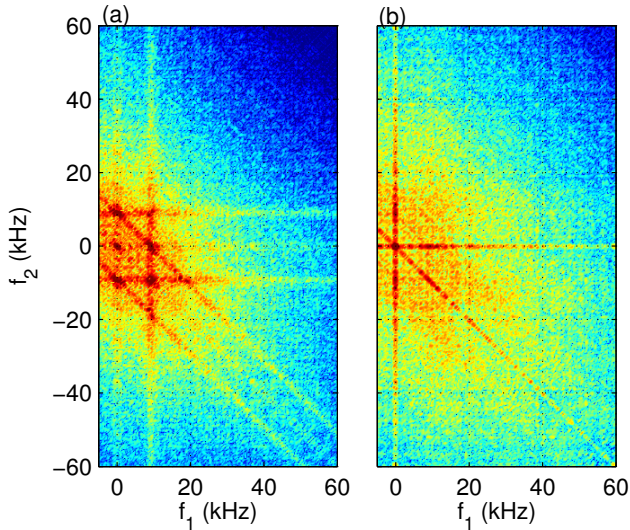


FIG. 5: Bispectra of potential fluctuations, for (a) shot 21856 $I_c = 0kA$ (b) shot 21857 $I_c = 1.4kA$, both for interval III

when the toroidal rotation reaches $M = \sqrt{2/5} = 0.63$ corresponding to a frequency of approximately 12 kHz. Thus a resonant transfer of energy from the GAM to the RMPs is possible, suppressing the build up of energy in the acoustic mode. We note however that we found no evidence of such coupling in the magnetics signals from the Mirnov coils. For the cases with slightly lower RMP level the decay of GAM appears to be more gradual in its temporal evolution. Examination of GAM peak decay times as a function of coil currents was attempted, but the probe was already pulling out of the plasma by the time the peak decreased significantly, thus no accurate estimate of damping time could be ascertained in these discharges.

Finally, we comment on the non-linear interactions between GAM and high frequency turbulence. We use a bispectrum, defined as $B_{f_3}(f_1, f_2) = \langle \phi(f_1)\phi(f_2)\phi^*(f_3) \rangle$, to measure the coherence of energy exchanged between different Fourier modes via a resonant three-wave interaction [25]. The resonant modes are those that fulfil the frequency relation $f_3 = f_1 + f_2$. Figure 5 shows the case without (a) and with (b) RMPs. We see that when the GAM peak is present in the spectrum strong non-linear and non-local (in k -space) interactions with the turbulence spectrum are dominant. These are represented by off-diagonal features on this plot. When the GAM peak is absent these features disappear and purely local cascade-like energy transfer is dominant. This coincides with the increased power level in the high frequency part of the spectrum, confirming a parasitic relation between GAM, as an energy sink, and turbulence.

In summary, we have reported a first observation of MHD potential fluctuations on MAST that are fully con-

sistent with the theoretical predictions derived for GAMs. The mode is radially localised, intermittent in time and is coupled to the high frequency turbulent spectrum. Resonant magnetic perturbations appear to have a dramatic impact on the GAM. Firstly, there is a shift upwards in frequency associated with the spin-up of the plasma. Secondly, the mode is suppressed entirely when the magnetic perturbations exceed a certain level. This can be interpreted as evidence that GAMs can indeed couple to the Alfvénic perturbations. The overall effect of such coupling would be detrimental to plasma confinement, since the dissipation of GAM increases the level of turbulent transport. We note that this apparent resonant suppression of GAM can be avoided if the toroidal rotation can be increased (to, say, $M \gtrsim 0.7$ in our case). This may be an important aspect of GAM dynamics that needs to be explored further, especially in the context of controlling the transition from a low to high confinement mode.

The Warwick team acknowledges EPSRC support (grant number EP/G02748X/1). This work was part-funded by the RCUK Energy Programme under grant EP/I501045 and the European Communities under the contract of Association between EURATOM and CCFE. The views and opinions expressed herein do not necessarily reflect those of the European Commission.

* Electronic address: James.Robinson@warwick.ac.uk

- [1] G. D. Conway, Plasma Phys. Control. Fusion **50**, 124026 (2008).
- [2] S. J. Zweben et al., Plasma Phys. Control. Fusion **49**, S1S23 (2007).
- [3] R. D. Hazeltine, J. D. Meiss, Plasma Confinement, Courier Dover Publications, 2003.
- [4] A. Hasegawa and M. Wakatani, Phys. Rev. Lett. **59**, 1581 (1987).
- [5] Z. Lin, T. S. Hahm, W. W. Lee, W. M. Tang, and R. B. White, Science **281**, 1835 (1998).
- [6] P. H. Diamond, S.-I. Itoh, K. Itoh, and T. S. Hahm, Plasma Phys. Control. Fusion **47**, R35 (2005).
- [7] M. Jakubowski, R. J. Fonck and G. R. McKee, Phys. Rev. Lett. **89**, 265003 (2002).
- [8] M. N. Rosenbluth and F. L. Hinton, Phys. Rev. Lett. **80**, 724727 (1998).
- [9] P. W. Terry, D. E. Newman, and A. S. Ware, Phys. Rev. Lett. **87** 185001 (2001).
- [10] R. A. Moyer, G. R. Tynan, C. Holland, and M. J. Burin, Phys. Rev. Lett. **87** 135001 (2001).
- [11] F. Wagner et al., Phys. Rev. Lett. **49**, 1408 (1982).
- [12] M. G. Shats, W. M. Solomon, and H. Xia, Phys. Rev. Lett. **90**, 125002 (2003).
- [13] N. Winsor, J. L. Johnson and J. M. Dawson, Phys. Fluids **11**, 2448 (1968).
- [14] G. D. Conway et al., Plasma Phys. Control. Fusion **47**, 1165 (2005).
- [15] D. K. Gupta et al., Phys. Rev. Lett. **97**, 125002 (2006).
- [16] A. I. Smolyakov, C. Nguyen and X. Garbet, Plasma Phys. Control. Fusion **50**, 115008 (2008).

- [17] A. Fujisawa et al., Phys. Plasmas **15**, 055906 (2008).
- [18] A. Kirk et al., Nucl. Fusion **50** 034008 (2010).
- [19] B. Lloyd et al., Nucl. Fusion **43**, 1665 (2003).
- [20] R. A. Moyer et al., Phys. Plasmas **2**, 2397 (1995).
- [21] C. S. MacLatchy et al, Rev. Sci. Instrum. **63**, 3923 (1992)
- [22] P. Tamain, et al., Plasma Phys. Control. Fusion **52**, 075017 (2010)
- [23] V. P. Lakhin, V. I. Ilgisonis, and A. I. Smolyakov, Phys Lett. A, **374** 4872 (2010)
- [24] D. Reiser, Phys. Plasmas **14**, 082314 (2007)
- [25] G. R. Tynan et al., Phys. Plasmas **8**, 2691 (2001).